

Catalysis by Orotidine 5'-Monophosphate Decarboxylase: Effect of 5-Fluoro and 4'-Substituents on the Decarboxylation of Two-Part Substrates

Bogdana Goryanova, Krisztina Spong, Tina L. Amyes, and John P. Richard*

Department of Chemistry, University at Buffalo, SUNY, Buffalo, New York 14260-3000, United States

ABSTRACT: The syntheses of two novel truncated analogs of the natural substrate orotidine 5'-monophosphate (OMP) for orotidine 5'-monophosphate decarboxylase (OMPDC) with enhanced reactivity toward decarboxylation are reported: 1-(β -D-erythrofuransyl)-5-fluoroorotic acid (FEO) and 5'-deoxy-5-fluoroorotidine (5'-dFO). A comparison of the second-order rate constants for the OMPDC-catalyzed decarboxylations of FEO ($10 \text{ M}^{-1} \text{ s}^{-1}$) and 1-(β -D-erythrofuransyl)orotic acid (EO, $0.026 \text{ M}^{-1} \text{ s}^{-1}$) shows that the vinyl carbanion-like transition state is stabilized by 3.5 kcal/mol by interactions with the 5-F substituent of FEO. The OMPDC-catalyzed decarboxylations of FEO and EO are both activated by exogenous phosphite dianion (HPO_3^{2-}), but the 5-F substituent results in only a 0.8 kcal stabilization of the transition state for the phosphite-activated reaction of FEO. This provides strong evidence that the phosphite-activated OMPDC-catalyzed reaction of FEO is not limited by the chemical step of decarboxylation of the enzyme-bound substrate. Evidence is presented that there is a change in the rate-limiting step from the chemical step of decarboxylation for the phosphite-activated reaction of EO, to closure of the phosphate gripper loop and an enzyme conformational change at the ternary $\text{E} \cdot \text{FEO} \cdot \text{HPO}_3^{2-}$ complex for the reaction of FEO. The 4'-CH₃ and 4'-CH₂OH groups of 5'-dFO and orotidine, respectively, result in identical destabilizations of the transition state for the unactivated decarboxylation of 2.9 kcal/mol. By contrast, the 4'-CH₃ group of 5'-dFO and the 4'-CH₂OH group of orotidine result in very different 4.7 and 8.3 kcal/mol destabilizations of the transition state for the phosphite-activated decarboxylation. Here, the destabilizing effect of the 4'-CH₃ substituent at 5'-dFO is masked by the rate-limiting conformational change that depresses the third-order rate constant for the phosphite-activated reaction of the parent substrate FEO.

		OMP Decarboxylase		
X	Y	k_{rel}	HPO_3^{2-} Effect	
H	H	1	7.7 kcal/mol	
F	H	400	5.0 kcal/mol	
H	CH ₂ OH	0.007	2.3 kcal/mol	
F	CH ₃	3	3.2 kcal/mol	

Orotidine 5'-monophosphate decarboxylase (OMPDC) employs no metal ions or other cofactors yet effects an enormous 10^{17} -fold acceleration of the decarboxylation of enzyme-bound orotidine 5'-monophosphate (OMP, Scheme 1A) to give uridine 5'-monophosphate (UMP).^{1,2} We have shown that the enzymatic reaction proceeds by a stepwise mechanism through a vinyl carbanion intermediate,^{3–6} and the overall rate acceleration corresponds to a 31 kcal/mol stabilization of the transition state by interactions of OMP with the protein catalyst.^{1,2} The functionalities present in the substrate OMP are, in principle, sufficient to account for this large transition state binding energy, but the mechanism for the increase in the stabilizing binding interactions with the protein from ca. 8 kcal/mol at the ground state Michaelis complex ($K_{\text{m}} = 1.4 \text{ } \mu\text{M}$)^{7,8} to 31 kcal/mol at the transition state for decarboxylation is poorly understood.^{9,10} This specificity in transition state binding is a feature of enzyme-catalyzed reactions that exhibit large transition state binding energies and is required to prevent the irreversible formation of tight Michaelis complexes with the reactant and/or product.

We have developed novel experimental protocols for study of the mechanism of action of OMPDC and have used these to characterize the enzyme specificity in binding the transition state as follows. First, we characterized the interactions between the phosphodianion group of OMP and OMPDC by evaluating the effect of removal of the 4'-CH₂OPO₃²⁻ group of OMP to

give the truncated neutral substrate 1-(β -D-erythrofuransyl)-orotic acid (EO, Scheme 1B). The second-order rate constant for OMPDC-catalyzed decarboxylation of EO is 4×10^8 -fold smaller than that for OMP, which shows that interactions of the protein with the 4'-CH₂OPO₃²⁻ group of OMP provide a ca. 12 kcal/mol stabilization of the transition state for decarboxylation.¹¹ However, these interactions do not simply anchor OMP to OMPDC, because ca. 8 kcal/mol of this phosphodianion binding energy is recovered as transition state stabilization from the binding of phosphite dianion (HPO_3^{2-}) to the transition state in the phosphite-activated decarboxylation of EO (Scheme 1B).^{7,11–13} The activation of OMPDC by phosphite dianion results from the high specificity of the dianion for binding to the transition state for the OMPDC-catalyzed decarboxylation of EO, compared with the weak binding of phosphite to the free enzyme ($K_{\text{d}} \approx 0.1 \text{ M}$).¹¹ We propose that OMPDC exhibits the same specificity for the tethered 4'-CH₂OPO₃²⁻ group of OMP so that the binding interactions of this substrate moiety are utilized for transition state stabilization.^{10,13}

Second, OMPDC was shown to provide effective catalysis of the exchange for deuterium of the C-6 protons of UMP and 5-

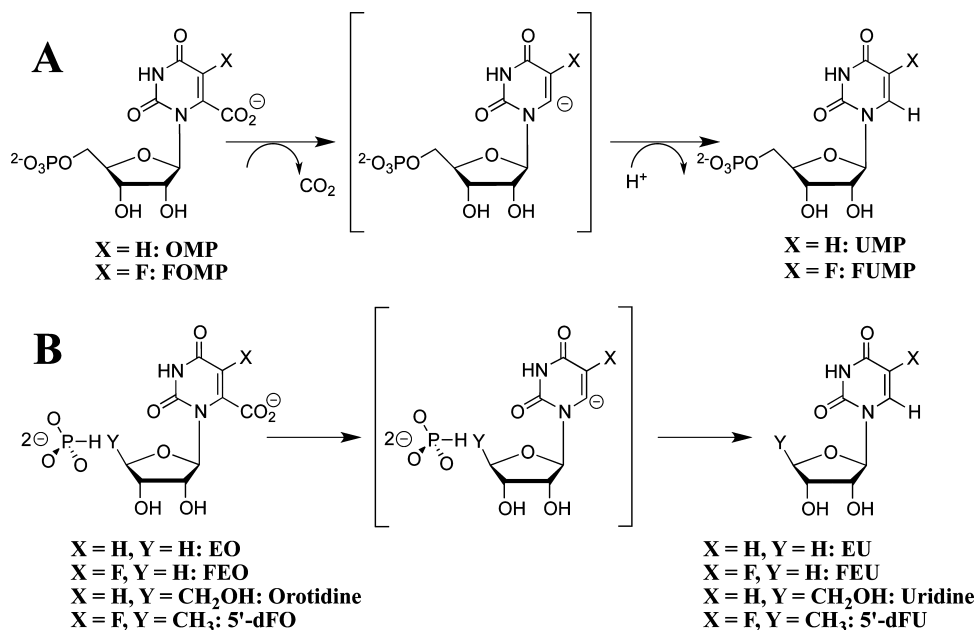
Received: December 11, 2012

Revised: December 29, 2012

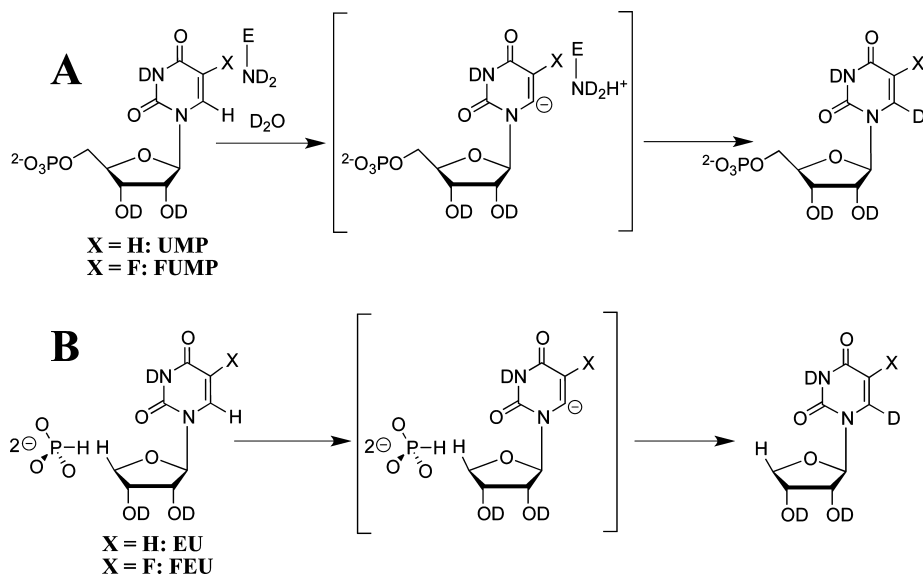
Published: December 31, 2012



Scheme 1



Scheme 2

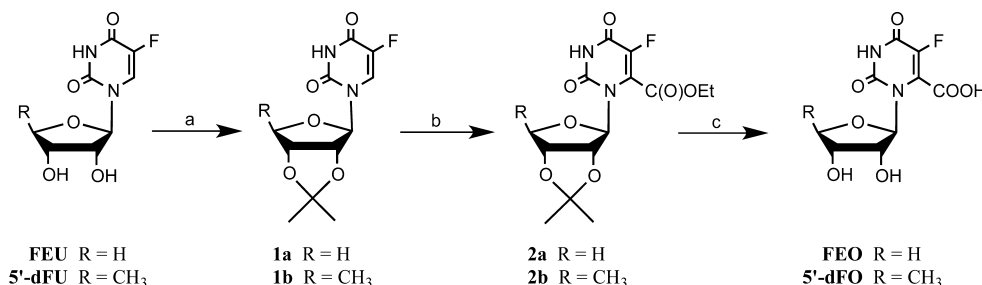


fluorouridine 5'-monophosphate (FUMP) in D_2O (Scheme 2A).^{3,5,14} The kinetic data for the enzymatic and nonenzymatic deuterium exchange reactions of UMP and FUMP show that OMPDC stabilizes the vinyl carbanion intermediate relative to the bound substrate by *at least* 13 kcal/mol.^{3,5} This strong stabilization of the UMP and FUMP vinyl carbanion intermediates (Scheme 2A) is reflected in the high *specificity* of OMPDC for binding the carbanion-like transition state of the enzyme-catalyzed deuterium exchange reactions.^{15,16}

Third, these protocols were combined in a study of the OMPDC-catalyzed exchange for deuterium of the C-6 proton of the *truncated* substrate 1-(β -D-erythrfuranosyl)-5-fluorouracil (FEU) in D_2O (Scheme 2B).¹⁷ The observed activation of this reaction by phosphite dianion shows that there is a large ca. 6 kcal/mol stabilization of the vinyl carbanion-like transition state by interactions with HPO_3^{2-} , which is similar to the ca. 8 kcal/mol stabilization of the transition state for the phosphite-

activated decarboxylation of EO.¹¹ We concluded that phosphite dianion exhibits the same high *specificity* for binding to the vinyl carbanion-like transition states that are common to the OMPDC-catalyzed decarboxylation and C-6 deuterium exchange reactions (Schemes 1B and 2B).

The addition of a 5-fluoro substituent to UMP to give FUMP results in a 3400-fold increase in the rate constant for the OMPDC-catalyzed C-6 deuterium exchange reaction of the enzyme-bound nucleotide in D_2O , as a result of stabilization of the negative charge at the vinyl carbanion intermediate by interaction with the electron-withdrawing 5-F substituent.^{3,5} By contrast, the stabilization of the vinyl carbanion-like transition state for the OMPDC-catalyzed decarboxylation of OMP by a 5-F substituent is not easily quantified, because the decarboxylation of 5-fluoroorotidine 5'-monophosphate (FOMP) is limited by substrate binding ($k_{\text{cat}}/K_{\text{m}}$) or product release (k_{cat}).¹⁸ We report here that the second-order rate

Scheme 3^a


^aReagents and conditions: (a) H_2SO_4 , acetone, room temperature, 1.5 h, ~90%; (b) (i) LDA, THF, -78°C , 2 h; (ii) EtOC(O)CN , THF, -78°C , 50 min, 70–75%; (c) (i) NaOH/THF, room temperature, 3 h; (ii) Dowex 50WX8–100 (H^+), H_2O , 45°C , 90–100%.

constant for the OMPDC-catalyzed decarboxylation of the novel truncated substrate 1-(β -D-erythrofuranosyl)-5-fluoroorotic acid (FEO, Scheme 1B) is 400-fold larger than that for the decarboxylation of EO. Surprisingly, we find that the third-order rate constant for the phosphite-activated decarboxylation of FEO is only 4-fold larger than that for the decarboxylation of EO. The obliteration of the 5-F substituent effect is attributed to a change in the rate-limiting step for the phosphite-activated reaction, from the chemical step of decarboxylation for EO to an obligate conformational change for the reaction of FEO.

We also report the effect of 4'-substituents on the kinetic parameters for the OMPDC-catalyzed decarboxylation reactions of EO and FEO. The addition of a 4'- CH_2OH group to EO to give orotidine or of a 4'- CH_3 group to FEO to give 5'-deoxy-5-fluoroorotidine (5'-dFO) results in identical destabilizations of the transition state for OMPDC-catalyzed decarboxylation of 2.9 kcal/mol. These surprisingly large 4'- CH_2OH and 4'- CH_3 substituent effects provide striking evidence that OMPDC-catalyzed decarboxylation proceeds through a transition state that is stabilized by a highly organized, but easily disrupted, network of protein–ligand interactions that extend from the substrate phosphodianion group to the pyrimidine binding loci at OMPDC.

EXPERIMENTAL SECTION

Materials. Orotidine 5'-monophosphate and 1-(β -D-erythrofuranosyl)-5-fluorouracil (FEU) were available from our earlier studies.^{4,7,17,19} 5'-Deoxy-5-fluorouridine (5'-dFU, 98%) was purchased from AK Scientific. Orotidine, 5-fluorouridine ($\geq 99.0\%$), ethyl cyanoformate (99%), diisopropylamine (redistilled, 99.95%), butyllithium (1.6 M solution in hexanes), and 3-(*N*-morpholino)propanesulfonic acid (MOPS, $\geq 99.5\%$) were purchased from Sigma-Aldrich. Sodium phosphite (dibasic, pentahydrate) was purchased from Riedel-de Haën (Fluka). Acetone was dried over calcium sulfate (CaSO_4) and distilled prior to use. Water was from a Milli-Q Academic purification system. All other chemicals were reagent grade or better and were used without further purification.

Wildtype orotidine 5'-monophosphate decarboxylase from *Saccharomyces cerevisiae* (OMPDC) was prepared as described previously.^{12,18} The protein sequence differs from the published sequence for wildtype yeast OMPDC by the following mutations: S2H, C155S, A160S, and N267D.^{12,18} The C155S mutation does not affect the kinetic parameters or the overall structure of the enzyme.²⁰

Chemical Syntheses. Our syntheses of the novel compounds 1-(β -D-erythrofuranosyl)-5-fluoroorotic acid (FEO) and 5'-deoxy-5-fluoroorotidine (5'-dFO) are summar-

ized in Scheme 3. Lithium diisopropylamide (LDA) was prepared from redistilled diisopropylamine and butyllithium (BuLi, 1.6 M solution in hexanes) by the following procedure: BuLi (2 mL, 3.2 mmol) was added slowly to a solution of diisopropylamine (0.5 mL, 3.6 mmol) in dry tetrahydrofuran (THF, 30 mL) under argon at -78°C . The solution was stirred under argon for 1 h at -78°C and the whole was used immediately as described below.

^1H and ^{19}F NMR spectra were acquired on a Varian Unity Inova 500 spectrometer operating at 500 MHz for proton. Proton chemical shifts (δ ppm) were referenced to the appropriate solvent peak: 4.69 ppm for HOD in D_2O , 2.54 ppm for DMSO- d_6 in DMSO- d_6 , and 7.26 ppm for CHCl_3 in CDCl_3 . Proton chemical shift assignments were confirmed using two-dimensional ^1H – ^1H correlated spectroscopy (^1H – ^1H COSY).

2',3'-O-Isopropylidene-1-(β -D-erythrofuranosyl)-5-fluorouracil (1a). The ribosyl hydroxyl groups of FEU and 5'-dFU were protected using adaptations of published procedures as follows.²¹ FEU (0.31 g, 1.34 mmol) was dried *in vacuo* over activated molecular sieves (4 Å) for 24 h at 50°C and then dissolved in dry acetone (22 mL). The reaction was initiated by the slow addition of concentrated H_2SO_4 (0.16 mL) under argon at 0°C . After 80 min at room temperature the solution was poured into saturated aqueous NaHCO_3 (10 mL), stirred for 25 min at room temperature, and extracted with chloroform (4 \times 30 mL). The combined organic extracts were dried (MgSO_4), and the solvent was removed by evaporation under reduced pressure to give 1a as a white solid (0.34 g, 1.25 mmol, 93%) which was used without further purification. ^1H NMR (500 MHz, CDCl_3) δ ppm: 9.16 (s, 1H, NH), 7.34 (d, 1H, $J_{\text{HF}} = 6$ Hz, C6–H), 5.39 (broad s, 1H, C1'–H), 5.18 (d, 1H, $J = 6$ Hz, C2'–H), 5.06 (dd, 1H, $J = 6, 4$ Hz, C3'–H), 4.33 (dd, 1H, $J = 10, 4$ Hz, C4'– H_A), 4.24 (d, 1H, $J = 10$ Hz, C4'– H_B), 1.56 (s, 3H, CH_3), 1.39 (s, 3H, CH_3).

5'-Deoxy-2',3'-O-isopropylidene-5-fluorouridine (1b). The procedure described above for the synthesis of 1a was followed for the preparation of 1b from 5'-dFU (0.67 g, 2.72 mmol). The yellow solid obtained from chloroform extraction was purified by flash chromatography on silica gel (hexanes/ethyl acetate 1:1) to give 1b as a white solid (0.70 g, 2.44 mmol, 90%): ^1H NMR (500 MHz, CDCl_3) δ ppm: 9.42 (s, 1H, NH), 7.39 (d, 1H, $J_{\text{HF}} = 6$ Hz, C6–H), 5.70 (d, 1H, $J = 2.5$ Hz, C1'–H), 4.9 (dd, 1H, $J = 6.5, 2.5$ Hz, C2'–H), 4.52 (dd, 1H, $J = 6.5, 4.5$ Hz, C3'–H), 4.27 (dq, 1H, $J = 6.5, 4.5$ Hz, C4'–H), 1.59 (s, 3H, CCH_3), 1.43 (d, 3H, $J = 6.5$ Hz, 4'- CH_3), 1.37 (s, 3H, CCH_3).

2',3'-O-Isopropylidene-1-(β -D-erythrofuranosyl)-5-fluoroorotic Acid Ethyl Ester (2a**).** Freshly prepared LDA (3.2 mmol) was added slowly to a solution of **1a** (0.34 g, 1.23 mmol) in dry THF (10 mL) under argon at -78°C . The mixture was stirred for 2 h at -78°C after which ethyl cyanofornate (0.5 mL, 5.06 mmol) was added. After 50 min the reaction was quenched with water (20 mL), stirred for 20 min at room temperature, followed by neutralization of residual HCN by the addition of solid Na_2CO_3 and extraction with ethyl acetate (4×30 mL). The combined organic extracts were dried (MgSO_4), and the solvent was removed by evaporation under reduced pressure to give a brown oil. Purification by flash chromatography on silica gel (hexanes/ethyl acetate 2:1) gave a yellow solid (0.33 g, 78%) which was recrystallized from hexanes/diethyl ether to give **2a** as a white solid (0.30 g, 70%): mp $159\text{--}161^{\circ}\text{C}$. ^1H NMR (500 MHz, CDCl_3) δ ppm: 8.68 (s, 1H, NH), 5.45 (d, 1H, $J = 0.5$ Hz, C1'-H), 5.26 (dd, 1H, $J = 6.5, 0.5$ Hz, C2'-H), 5.09 (m, 1H, C3'-H), 4.52 (q, 2H, $J = 7$ Hz, CH_2CH_3), 4.44 (dd, 1H, $J = 10, 4$ Hz, C4'-H_A), 4.15 (d, 1H, $J = 10$ Hz, C4'-H_B), 1.53 (s, 3H, CCH_3), 1.45 (t, 3H, $J = 7$ Hz, CH_2CH_3), 1.38 (s, 3H, CCH_3). HRMS (ESI): calculated $(\text{M} + \text{Na})^+ \text{C}_{14}\text{H}_{17}\text{O}_7\text{N}_2\text{FNa}$, 367.0912; found, 367.0908.

5'-Deoxy-2',3'-O-isopropylidene-5-fluororotidine Ethyl Ester (2b**).** The procedure described above for the preparation of **2a** was followed for the preparation of **2b** from **1b** (0.34 g, 1.33 mmol). The crude product, a dark brown oil, was purified by flash chromatography on silica gel (hexanes/ethyl acetate 2:1) to give a yellow solid (0.39 g, 82%). Recrystallization from hexanes/diethyl ether gave **2b** as a white solid (0.36 g, 75%): mp $146\text{--}147^{\circ}\text{C}$. ^1H NMR (500 MHz, CDCl_3) δ ppm: 9.23 (s, 1H, NH), 5.75 (d, 1H, $J = 2.5$ Hz, C1'-H), 5.17 (dd, 1H, $J = 6.5, 2.5$ Hz, C2'-H), 4.52 (m, 2H, C3'-H and CH_2CH_3), 4.42 (m, 1H, CH_2CH_3), 4.07 (m, 1H, C4'-H), 1.58 (s, 3H, CCH_3), 1.44 (t, 3H, $J = 7$ Hz, CH_2CH_3), 1.38 (d, 3H, $J = 6.5$ Hz, 4'- CH_3), 1.37 (s, 3H, CCH_3). HRMS (ESI): calculated $(\text{M} + \text{Na})^+ \text{C}_{15}\text{H}_{19}\text{O}_7\text{N}_2\text{FNa}$, 381.1069; found, 381.1079.

1-(β -D-Erythrofuranosyl)-5-fluoroorotic Acid (FEO). The hydrolyses of the ethyl ester groups of **2a** and **2b** were carried out in THF containing NaOH. The failure to allow the hydrolysis of **2a** to proceed to completion resulted in poor product yields in the subsequent removal of the isopropylidene group. Therefore, the reaction time was optimized by monitoring a small scale reaction in d_8 -THF by ^1H NMR, for which the ester hydrolysis was judged to be complete after 2.5 h at room temperature.

2a (132 mg, 0.38 mmol) was dissolved in 2.7 mL of THF and 0.54 mL of 3 M NaOH was added with stirring at room temperature.²² After 3 h at room temperature the solution was poured into a mixture of 4 mL water and 10 mL of wet Dowex 50WX8-100 (H^+) and stirred for 3 h at room temperature followed by 3 h at 45°C . The Dowex resin was removed by filtration and washed with water (3×20 mL), and the combined aqueous extracts were lyophilized to give FEO as a white solid (104 mg, 0.38 mmol, 100%): mp $212\text{--}214^{\circ}\text{C}$. ^1H NMR (500 MHz, D_2O) δ ppm: 5.60 (d, 1H, $J = 6$ Hz, C1'-H), 4.57 (dd, 1H, $J = 6, 5$ Hz, C2'-H), 4.29 (m, 1H, C3'-H), 4.24 (dd, 1H, $J = 10, 3.5$ Hz, C4'-H_A), 3.84 (dd, 1H, $J = 10$ Hz, 1.5 Hz, C4'-H_B). ^{19}F NMR (470 MHz, D_2O) δ ppm: -169.46 (s, 1F, C5-F). HRMS (ESI): calculated $(\text{M} + 2\text{Na})^{2+} \text{C}_9\text{H}_8\text{O}_7\text{N}_2\text{FNa}_2$, 321.0105; found, 321.0100.

5'-Deoxy-5-fluoroorotidine (5'-dFO). The procedure described above for the preparation of FEO was followed for the preparation of 5'-dFO from **2b** (0.040 g, 0.11 mmol), except

that removal of the isopropylidene protecting group using Dowex (H^+) employed a 16 h reaction time at 45°C . This gave 5'-dFO as a white solid (0.045 g, 0.10 mmol, 90%). ^1H NMR (500 MHz, D_2O) δ ppm: 5.33 (d, 1H, $J = 2.5$ Hz, C1'-H), 4.57 (dd, 1H, $J = 6, 2.5$ Hz, C2'-H), 3.99 (m, 1H, C3'-H), 3.80 (m, 1H, C4'-H), 1.26 (d, 3H, $J = 6.5$ Hz, 4'- CH_3). ^{19}F NMR (470 MHz, D_2O) δ ppm: -169.61 (s, 1F, C5-F). HRMS (ESI): calculated $(\text{M} - 1)^- \text{C}_{10}\text{H}_{10}\text{O}_7\text{N}_2\text{F}$, 289.0478; found, 289.0478.

Kinetic Studies. Preparation of Solutions. Solution pH was determined at 25°C using an Orion model 720A pH meter equipped with a Radiometer pHC4006-9 combination electrode that was standardized at pH 7.00 and 10.00 at 25°C . Stock solutions of OMP, FEO, 5'-dFO, and orotidine were prepared by dissolution in water followed by adjustment to pH ≈ 7 using 1.0 M NaOH. The stock solution of 5'-dFO was freed of small amounts of contaminating 5'-dFU ($\leq 1\%$) by passage over Supelclean LC-18 solid phase extraction tubes (3 mL, Supelco), eluting with water. The solutions were stored at -20°C . The concentrations of FEO and 5'-dFO were determined from the absorbance in 0.1 M HCl at 271 nm using $\epsilon = 10200 \text{ M}^{-1} \text{ cm}^{-1}$ reported for FOMP.⁴ The concentrations of OMP and orotidine were determined from the absorbance in 0.1 M HCl at 267 nm using $\epsilon = 9430 \text{ M}^{-1} \text{ cm}^{-1}$ for OMP and $\epsilon = 9570 \text{ M}^{-1} \text{ cm}^{-1}$ for orotidine.²³

Stock solutions of sodium phosphite at pH 7.0 (80% dianion) were prepared by addition of a measured amount of 1 M HCl to the sodium salt to give the desired acid/base ratio. MOPS buffers at pH 7.0 (45% free base) or pH 7.1 (50% free base) were prepared by addition of measured amounts of 1 M NaOH and solid NaCl to give the desired acid/base ratio and ionic strength.

Samples of yeast OMPDC that had been stored at -80°C were defrosted and exhaustively dialyzed at 7°C against 50 mM MOPS (45% free base) at pH 7.0 and $I = 0.14$ (NaCl) for the experiments with FEO and 5'-dFO, or 100 mM MOPS (50% free base) at pH 7.1 and $I = 0.28$ (NaCl) for the experiments with orotidine. The concentration of OMPDC was determined from the absorbance at 280 nm using an extinction coefficient of $29910 \text{ M}^{-1} \text{ cm}^{-1}$, calculated using the ProtParam tool available on the ExPASy server.²⁴

Standard Enzyme Assays. The activity of OMPDC in the enzyme stock solutions and in the decarboxylation reaction mixtures was determined by monitoring the decrease in absorbance at 279 nm accompanying the enzyme-catalyzed decarboxylation of OMP ($\Delta\epsilon = -2400 \text{ M}^{-1} \text{ cm}^{-1}$ at 25°C).^{3,7,8,12} Prior to assay, the stock solutions of OMPDC were diluted with 10 mM MOPS, 50% free base (pH 7.1) containing 100 mM NaCl to give a final concentration of ca. 20 μM OMPDC. Assays in a total volume of 1 mL were conducted in 10 mM MOPS (50% free base) at pH 7.1, 25°C and $I = 0.105$ (NaCl), with 40–50 μM OMP ($25 - 30 K_m$). Reactions were initiated by the addition of 1 μL of the diluted stock solution of OMPDC or an aliquot of the decarboxylation reaction mixture to give a final enzyme concentration of 20–40 nM, and the initial velocity of the ensuing decarboxylation of OMP was determined within 1 min.

Yeast OMPDC-Catalyzed Decarboxylation of FEO. The decarboxylation of FEO catalyzed by OMPDC at pH 7.0, 25°C and $I = 0.14$ (NaCl) was followed spectrophotometrically by monitoring the decrease in absorbance at 282 nm.¹¹ Reactions in the absence of phosphite were initiated by the addition of 100 μL of enzyme to give a reaction mixture (1 mL) containing

25 mM MOPS (45% free base, pH 7.0), 0.14 mM FEO and 30 μ M OMPDC at $I = 0.14$ (NaCl). Reactions in the presence of phosphite were initiated by the addition of 10–100 μ L of enzyme to give reaction mixtures (1 mL) at pH 7.0 containing 5 mM MOPS (45% free base), 2–36 mM HPO_3^{2-} , 0.14 mM FEO, and 2.7–29 μ M OMPDC at $I = 0.14$ (NaCl). The reactions were monitored for 200–800 min (≥ 10 halftimes), after which standard assay (see above) showed that OMPDC maintained full activity toward decarboxylation of OMP. In several cases, after completion of the reaction, the enzyme was removed by ultrafiltration (Amicon, 10K MWCO) and the pH of the filtrate was determined. No change in pH was observed during these reactions.

Observed first-order rate constants for enzyme-catalyzed decarboxylation, k_{obs} (s^{-1}), were obtained from the fits of the progress curves to an equation for a single exponential decay.¹¹ The observed second-order rate constants ($k_{\text{cat}}/K_{\text{m}})_{\text{obs}}$ ($\text{M}^{-1} \text{s}^{-1}$) were calculated using the relationship ($k_{\text{cat}}/K_{\text{m}})_{\text{obs}} = k_{\text{obs}}/[E]$.

Yeast OMPDC-Catalyzed Decarboxylation of 5'-dFO. The decarboxylation of 5'-dFO catalyzed by OMPDC at pH 7.0, 25 °C and $I = 0.14$ (NaCl) was followed in a discontinuous assay in which the initial velocity of formation of the product 5'-dFU was monitored by HPLC analysis with peak detection at 270 nm, as described previously for the decarboxylation of EO.¹³ Reaction mixtures (200 μ L) were prepared by mixing stock solutions of the enzyme in MOPS buffer with stock solutions of MOPS buffer, sodium chloride and, if needed, sodium phosphite (100 mM, 80% dianion), and the reactions were initiated by the addition of an aliquot of the stock solution of 5'-dFO in water. The reaction conditions in the absence of phosphite dianion were 25 mM MOPS (45% free base, pH 7.0), 0.9–9 mM 5'-dFO and 65 μ M OMPDC at $I = 0.14$ (NaCl). The reaction conditions in the presence of phosphite dianion were 5 mM MOPS (45% free base, pH 7.0), 4–32 mM HPO_3^{2-} , 4.4 mM 5'-dFO and 10–50 μ M OMPDC at $I = 0.14$ (NaCl). The reactions were followed for up to 3 h, during which time there was up to ca. 5% reaction. At various times an aliquot (20 μ L) was withdrawn and the reaction was quenched by the addition of 180 μ L of a quench solution of formic acid (2.4 mM) containing ca. 60 μ M 5-fluorouracil that served as an internal standard. The enzyme was removed by ultrafiltration using an Amicon Ultra device (10K MWCO) that had been prewashed 2–3 times with 500 μ L of water. Failure to prewash the filtration device resulted in loss of retention and/or erratic HPLC retention times. The filtrate (100 μ L) was analyzed by HPLC using a Waters Atlantis dC₁₈ 3 μ m column (3.9 \times 150 mm) with a linear gradient from 10 mM NH_4OAc pH 4.2 to 60/40 $\text{NH}_4\text{OAc}/\text{MeOH}$ over 10 min, with a flow of 1 mL/min and peak detection at 270 nm. Under these conditions the unreacted 5'-dFO eluted at 2.5 min, 5-fluorouracil eluted at 4.2 min, and the product 5'-dFU eluted at 11.8 min. The observed HPLC peak area for 5'-dFU was normalized using the observed peak area for 5-fluorouracil, and the standard HPLC peak area for 5-fluorouracil was determined by direct HPLC analysis of the formic acid/5-fluorouracil quench solution. This procedure was necessary because there is a small variable dilution of the sample upon its passage through the prewashed filtration device. The concentration of the product 5'-dFU in the reaction mixture at time t , $[5'\text{-dFU}]_t$, was then obtained from its normalized HPLC peak area by interpolation of a standard curve that was constructed using 5-fluorouridine. The concentration of 5-fluorouridine in the stock solutions used

for this calibration was determined from the absorbance in 0.1 M HCl at 270 nm using $\epsilon = 9660 \text{ M}^{-1} \text{cm}^{-1}$ reported for FEU.¹⁷ Periodic standard assay of the reaction mixture using OMP as substrate (see above) showed that there was no significant decrease in the activity of OMPDC during these reactions.

Initial velocities of the decarboxylation of 5'-dFO, v_o (M s^{-1}), were determined as the slopes of linear plots of $[5'\text{-dFU}]_t$ against time that covered up to 5% reaction. The observed second-order rate constants ($k_{\text{cat}}/K_{\text{m}})_{\text{obs}}$ ($\text{M}^{-1} \text{s}^{-1}$) were determined using the relationship ($k_{\text{cat}}/K_{\text{m}})_{\text{obs}} = v_o/[E][5'\text{-dFO}]_o$, where $[5'\text{-dFO}]_o$ is the concentration of 5'-dFO at zero time.

Yeast OMPDC-Catalyzed Decarboxylation of Orotidine. The decarboxylation of orotidine catalyzed by OMPDC at pH 7.1, 25 °C and $I = 0.14$ or 0.21 (NaCl) was followed in a discontinuous assay in which the initial velocity of formation of the product uridine was monitored by HPLC analysis with peak detection at 262 nm.¹¹ Reaction mixtures (160 μ L) were prepared by mixing stock solutions of the enzyme in MOPS buffer with water and, if needed, sodium phosphite (200 mM, 80% dianion), and the reactions were initiated by the addition of an aliquot of the stock solution of orotidine in water. The reaction conditions in the absence of phosphite dianion were 50 mM MOPS (50% free base, pH 7.1), 10.3 mM orotidine, and 137 μ M OMPDC at $I = 0.14$ (NaCl). The reaction conditions in the presence of phosphite dianion were 25 mM MOPS (50% free base, pH 7.1), 40 mM HPO_3^{2-} , 10.3 mM orotidine, and 73 μ M OMPDC at $I = 0.21$ (NaCl). The reactions were followed for ca. 30 h, during which time there was ca. 0.5% reaction. At various times an aliquot (20 μ L) was withdrawn, and the reaction was quenched by the addition of 180 μ L of a quench solution of formic acid (6–12 mM). The enzyme was removed by ultrafiltration and the sample was analyzed by HPLC, as described previously for the decarboxylation of EO.¹¹ The concentration of the product uridine in the reaction mixture at time t , $[\text{uridine}]_t$, was obtained from the HPLC peak area by interpolation of a standard curve. Periodic standard assay of the reaction mixture using OMP as substrate (see above) showed that there was no significant decrease in the activity of OMPDC during these reactions.

Initial velocities of the decarboxylation of orotidine were determined as the slopes of linear plots of $[\text{uridine}]_t$ against time that covered up to 0.5% reaction. The observed second-order rate constants ($k_{\text{cat}}/K_{\text{m}})_{\text{obs}}$ ($\text{M}^{-1} \text{s}^{-1}$) were determined using the relationship ($k_{\text{cat}}/K_{\text{m}})_{\text{obs}} = v_o/[E][\text{orotidine}]_o$, where $[\text{orotidine}]_o$ is the concentration of orotidine at zero time.

RESULTS

The novel compounds FEO and 5'-dFO were synthesized in good yields using the procedures outlined in Scheme 3. These syntheses represent a novel approach to nucleosides containing a 5-fluoroorotate base.

The relatively rapid yeast OMPDC-catalyzed decarboxylation reactions of FEO (0.14 mM) to give FEU at pH 7.0, 25 °C and $I = 0.14$ (NaCl) in the absence and presence of phosphite dianion were followed spectrophotometrically by monitoring the decrease in absorbance at 282 nm. These reactions were clearly first-order for the entire reaction time course (≥ 10 halftimes). Observed first-order rate constants for enzyme-catalyzed decarboxylation, k_{obs} (s^{-1}), were obtained from the fits of the data to a single exponential.¹¹ The observed second-order rate constants, ($k_{\text{cat}}/K_{\text{m}})_{\text{obs}}$ ($\text{M}^{-1} \text{s}^{-1}$), were calculated

using the relationship $(k_{\text{cat}}/K_{\text{m}})_{\text{obs}} = k_{\text{obs}}/[\text{E}]$. The second-order rate constant for the OMPDC-catalyzed decarboxylation of FEO in the absence of phosphite dianion was determined as $(k_{\text{cat}}/K_{\text{m}})_{\text{E}} = 10 \text{ M}^{-1} \text{ s}^{-1}$ (Scheme 4).

Scheme 4

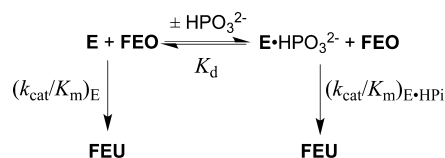


Figure 1A shows the dependence of the observed second-order rate constant $(k_{\text{cat}}/K_{\text{m}})_{\text{obs}}$ for OMPDC-catalyzed

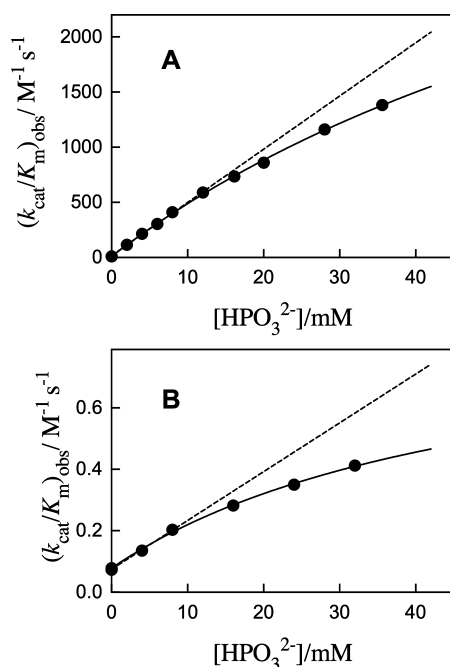


Figure 1. Dependence of the observed second-order rate constant for the yeast OMPDC-catalyzed decarboxylation of truncated substrates on the concentration of added phosphite dianion at pH 7.0, 25 °C and $I = 0.14$ (NaCl). (A) Decarboxylation of FEO. The solid line shows the fit of the data to eq 1, derived for Scheme 4, with $(k_{\text{cat}}/K_{\text{m}})_{\text{E}} = 10 \text{ M}^{-1} \text{ s}^{-1}$ and $K_{\text{d}} = 0.1 \text{ M}$. The dashed line is the linear correlation at $[\text{HPO}_3^{2-}] \leq 12 \text{ mM}$, the slope of which gives the third-order rate constant $(k_{\text{cat}}/K_{\text{m}})_{\text{E} \cdot \text{HPi}}/K_{\text{d}} = 4.8 \times 10^4 \text{ M}^{-2} \text{ s}^{-1}$. (B) Decarboxylation of 5'-dFO. The solid line shows the fit of the data to eq 1 with $(k_{\text{cat}}/K_{\text{m}})_{\text{E}} = 0.078 \text{ M}^{-1} \text{ s}^{-1}$ and $K_{\text{d}} = 0.05 \text{ M}$. The dashed line is the linear correlation at $[\text{HPO}_3^{2-}] \leq 8 \text{ mM}$, the slope of which gives the third-order rate constant $(k_{\text{cat}}/K_{\text{m}})_{\text{E} \cdot \text{HPi}}/K_{\text{d}} = 16 \text{ M}^{-2} \text{ s}^{-1}$.

decarboxylation of FEO on the concentration of added phosphite dianion at pH 7.0, 25 °C and a constant ionic strength of 0.14 (NaCl). There is weak downward curvature at high concentrations of phosphite, which is consistent with partial saturation of the enzyme by HPO_3^{2-} to give the $\text{E} \cdot \text{HPO}_3^{2-}$ complex (Scheme 4). The solid line shows the nonlinear least-squares fit of the data to eq 1, derived for Scheme 4, with $(k_{\text{cat}}/K_{\text{m}})_{\text{E}} = 10 \text{ M}^{-1} \text{ s}^{-1}$, which gave $K_{\text{d}} = 0.1 \text{ M}$ for binding of phosphite to OMPDC, and $(k_{\text{cat}}/K_{\text{m}})_{\text{E} \cdot \text{HPi}} = 5000 \text{ M}^{-1} \text{ s}^{-1}$ for decarboxylation catalyzed by the phosphite-liganded enzyme $\text{E} \cdot \text{HPO}_3^{2-}$ (Scheme 4). However, it is also possible that the downward curvature results from a specific salt

effect arising from the replacement of Cl^- with HPO_3^{2-} .⁷ Therefore, the third-order rate constant for the phosphite-activated reaction of FEO was determined as the slope of the linear correlation of the data at $[\text{HPO}_3^{2-}] \leq 12 \text{ mM}$, as $(k_{\text{cat}}/K_{\text{m}})_{\text{E} \cdot \text{HPi}}/K_{\text{d}} = 4.8 \times 10^4 \text{ M}^{-2} \text{ s}^{-1}$. Table 1 reports the rate

Table 1. Kinetic Parameters for the Decarboxylation of Truncated Substrates Catalyzed by Yeast OMPDC and for Activation by Phosphite Dianion at 25 °C^a

	EO	FEO	orotidine	5'-dFO
$(k_{\text{cat}}/K_{\text{m}})_{\text{E}}^b$ ($\text{M}^{-1} \text{ s}^{-1}$)	0.026 ^c	10	1.8×10^{-4d}	0.078
$(k_{\text{cat}}/K_{\text{m}})_{\text{E} \cdot \text{HPi}}/K_{\text{d}}^e$ ($\text{M}^{-2} \text{ s}^{-1}$)	1.2×10^{4f}	4.8×10^4	9.3×10^{-3g}	16
activation by 1 M HPO_3^{2-}	5×10^5 -fold	5×10^3 -fold	50-fold	200-fold
intrinsic phosphite binding energy (kcal/mol)	7.7	5.0	2.3	3.2

^aAt pH 7.0 and $I = 0.14$ (NaCl), unless noted otherwise. ^bSecond-order rate constant for the unactivated OMPDC-catalyzed decarboxylation of the truncated substrate in the absence of phosphite. The estimated error is $\pm 10\%$. ^cData from ref 13. ^dAt pH 7.1. ^eThird-order rate constant for the phosphite-activated OMPDC-catalyzed decarboxylation of the truncated substrate. The estimated error is $\pm 20\%$. ^fData from ref 11. ^gAt pH 7.1 and $I = 0.21$ (NaCl).

constants for the unactivated and phosphite-activated reactions of FEO that were determined in these experiments.

$$\begin{aligned} \left(\frac{k_{\text{cat}}}{K_{\text{m}}} \right)_{\text{obs}} &= \left(\frac{K_{\text{d}}}{K_{\text{d}} + [\text{HPO}_3^{2-}]} \right) \left(\frac{k_{\text{cat}}}{K_{\text{m}}} \right)_{\text{E}} \\ &+ \left(\frac{[\text{HPO}_3^{2-}]}{K_{\text{d}} + [\text{HPO}_3^{2-}]} \right) \left(\frac{k_{\text{cat}}}{K_{\text{m}}} \right)_{\text{E} \cdot \text{HPi}} \end{aligned} \quad (1)$$

The initial velocities, v_o (M s^{-1}), of the yeast OMPDC-catalyzed decarboxylation of 5'-dFO (up to 9 mM) at pH 7.0, 25 °C and $I = 0.14$ (NaCl) were determined by following the formation of up to 5% of the product 5'-dFU by HPLC. Observed second-order rate constants were determined using the relationship $(k_{\text{cat}}/K_{\text{m}})_{\text{obs}} = v_o/[\text{E}][\text{5'-dFO}]_o$, where $[\text{5'-dFO}]_o$ is the concentration of 5'-dFO at zero time. The second-order rate constant for the OMPDC-catalyzed decarboxylation of 5'-dFO in the absence of phosphite dianion was determined as $(k_{\text{cat}}/K_{\text{m}})_{\text{E}} = 0.078 \text{ M}^{-1} \text{ s}^{-1}$ (Scheme 4). There was no significant change in the value of $(k_{\text{cat}}/K_{\text{m}})_{\text{E}}$ when the concentration of 5'-dFO was increased from 0.9 to 9 mM, which shows that there is no significant saturation of OMPDC by 9 mM 5'-dFO.¹¹

Figure 1B shows the dependence of the observed second-order rate constant $(k_{\text{cat}}/K_{\text{m}})_{\text{obs}}$ for OMPDC-catalyzed decarboxylation of 5'-dFO on the concentration of added phosphite dianion at pH 7.0, 25 °C and a constant ionic strength of 0.14 (NaCl). The modest downward curvature is consistent with $K_{\text{d}} = 0.050 \text{ M}$ (Scheme 4). The third-order rate constant for the phosphite-activated reaction of 5'-dFO was determined as the slope of the linear correlation of the data at $[\text{HPO}_3^{2-}] \leq 8 \text{ mM}$, as $(k_{\text{cat}}/K_{\text{m}})_{\text{E} \cdot \text{HPi}}/K_{\text{d}} = 16 \text{ M}^{-2} \text{ s}^{-1}$. Table 1 reports the rate constants for the unactivated and phosphite-activated reactions of 5'-dFO that were determined in these experiments.

The second-order rate constant for the yeast OMPDC-catalyzed decarboxylation of orotidine to give uridine at pH 7.1,

25 °C and $I = 0.14$ (NaCl) in the absence of phosphite dianion was determined by our HPLC assay as $(k_{\text{cat}}/K_{\text{m}})_{\text{E}} = 1.8 \times 10^{-4} \text{ M}^{-1} \text{ s}^{-1}$ (Table 1). This is in good agreement with the earlier value of $2 \times 10^{-4} \text{ M}^{-1} \text{ s}^{-1}$ determined under similar conditions by following the release of $^{14}\text{CO}_2$ that accompanies the decarboxylation of orotidine labeled at the 6-CO_2^- group.²⁰ The observed second-order rate constant for the decarboxylation of orotidine in the presence of 40 mM phosphite dianion at pH 7.0, 25 °C and $I = 0.21$ (NaCl) was determined as $(k_{\text{cat}}/K_{\text{m}})_{\text{obs}} = 5.6 \times 10^{-4} \text{ M}^{-1} \text{ s}^{-1}$. This was used to estimate the third-order rate constant for the phosphite-activated reaction of orotidine as $(k_{\text{cat}}/K_{\text{m}})_{\text{E}\cdot\text{HPi}}/K_{\text{d}} = [(k_{\text{cat}}/K_{\text{m}})_{\text{obs}} - (k_{\text{cat}}/K_{\text{m}})_{\text{E}}]/0.04 = 9.3 \times 10^{-3} \text{ M}^{-2} \text{ s}^{-1}$ (Table 1).

DISCUSSION

We showed previously that a comparison of the effects of site-directed mutations of OMPDC on the kinetic parameters for decarboxylation of the whole substrate **OMP** and on the decarboxylation of the truncated substrate **EO** activated by the second substrate piece HPO_3^{2-} allows for a clean distinction between the amino acid side chains at OMPDC that interact with the substrate phosphodianion and those that interact with the pyrimidine ring.^{12,13} However, the severity of the mutations that can be examined is limited by the low reactivity of the truncated substrate **EO**, for which the second-order rate constant for unactivated decarboxylation catalyzed by wildtype yeast OMPDC is $(k_{\text{cat}}/K_{\text{m}})_{\text{E}} = 0.026 \text{ M}^{-1} \text{ s}^{-1}$.^{11,13} The desire to characterize an expanded range of mutations prompted us to develop a synthesis of the more reactive 5-fluoro substituted truncated substrate **FEO** (Scheme 3). The high reactivity of this substrate in enzyme-catalyzed decarboxylation has enabled the study of severely impaired site-directed mutants of OMPDC from *Methanothermobacter thermautotrophicus*, which show extremely low activities for the decarboxylation of **EO**.²⁵

5-Fluoro Substituent Effects. The addition of a 5-F substituent to **EO** to give **FEO** results in a 390-fold increase in the second-order rate constant for the unactivated yeast OMPDC-catalyzed decarboxylation through a carbanion intermediate (Scheme 1B), from $(k_{\text{cat}}/K_{\text{m}})_{\text{E}} = 0.026 \text{ M}^{-1} \text{ s}^{-1}$ for **EO** to $10 \text{ M}^{-1} \text{ s}^{-1}$ for **FEO** (Tables 1 and 2). Therefore, the 5-F substituent provides a 3.5 kcal/mol stabilization of the carbanion-like transition state for enzyme-catalyzed decarbox-

ylation (Table 2), which suggests that the *chemical* step of decarboxylation of the enzyme-bound substrate to give the enzyme-bound product **EU** or **FEU** is clearly rate-determining for these reactions. Similarly, the addition of a 5-F substituent to **UMP** to give **FUMP** results in a 3400-fold increase in the rate constant for the OMPDC-catalyzed C-6 deuterium exchange reaction of the enzyme-bound nucleotide in D_2O (Scheme 2A),^{3,5} so that the negative charge in the transition state for formation of the vinyl carbanion intermediate is stabilized by 4.8 kcal/mol by interactions with the 5-F substituent (Table 2). These substituent effects on decarboxylation and deuterium exchange provide a measure of the *change* in the interactions of the reacting center with the 5-F substituent on proceeding from the reactant to the carbanion-like transition state in each case.²⁶ The effect of a 5-F substituent on the OMPDC-catalyzed decarboxylation of **OMP** is ca. 1 kcal/mol smaller than that on the deuterium exchange reaction of **UMP** (Table 2). This suggests that the *gain* in the stabilizing interactions of the developing negative charge with the 5-F substituent on proceeding to the transition state for decarboxylation is partly offset by the *loss* of *ground state* stabilizing interactions of the 5-F substituent with the anionic 6-CO_2^- group of the substrate.

The very similar kinetic parameters for the yeast OMPDC-catalyzed decarboxylation reactions of the natural substrate **OMP** ($k_{\text{cat}}/K_{\text{m}} = 1.1 \times 10^7 \text{ M}^{-1} \text{ s}^{-1}$, $k_{\text{cat}} = 15 \text{ s}^{-1}$)⁷ and of the 5-F substituted substrate **FOMP** ($k_{\text{cat}}/K_{\text{m}} = 1.2 \times 10^7 \text{ M}^{-1} \text{ s}^{-1}$, $k_{\text{cat}} = 95 \text{ s}^{-1}$)²⁷ show that there is little or no effect of a 5-F substituent on the stability of the transition state for decarboxylation of the natural substrate (Scheme 1A). The formation of the Michaelis complex is partly rate-determining for $k_{\text{cat}}/K_{\text{m}}$ for turnover of **OMP** by yeast OMPDC,⁸ so that these essentially identical large values of $k_{\text{cat}}/K_{\text{m}}$ for decarboxylation of **OMP** and the chemically more reactive **FOMP** are consistent with cleanly rate-determining formation of the productive Michaelis complex for **FOMP**, with a second-order rate constant $k_{\text{d}} = k_{\text{cat}}/K_{\text{m}} \approx 10^7 \text{ M}^{-1} \text{ s}^{-1}$ (Scheme 5).

Scheme 5

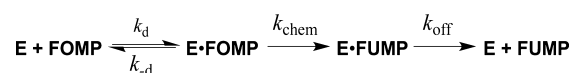


Table 2. Effect of a 5-Fluoro Substituent on Decarboxylation and C-6 Deuterium Exchange Reactions Catalyzed by Yeast OMPDC at 25 °C

substrate	reaction	rate constant	effect of 5-F substituent	$\Delta\Delta G^\ddagger$ (kcal/mol)
OMP	decarboxylation	$k_{\text{cat}}/K_{\text{m}}$ ($\text{M}^{-1} \text{ s}^{-1}$)	none ^a	0
EO	decarboxylation	$(k_{\text{cat}}/K_{\text{m}})_{\text{E}}$ ($\text{M}^{-1} \text{ s}^{-1}$)	+ 390-fold ^b	−3.5
EO + HPO_3^{2-}	decarboxylation	$(k_{\text{cat}}/K_{\text{m}})_{\text{E}\cdot\text{HPi}}/K_{\text{d}}$ ($\text{M}^{-2} \text{ s}^{-1}$)	+ 4-fold ^b	−0.8
UMP	exchange	k_{ex} (s^{-1})	+ 3400-fold ^c	−4.8

^aCalculated from the values of $k_{\text{cat}}/K_{\text{m}}$ for the decarboxylation reactions of **OMP** ($1.1 \times 10^7 \text{ M}^{-1} \text{ s}^{-1}$, ref 7) and **FOMP** ($1.2 \times 10^7 \text{ M}^{-1} \text{ s}^{-1}$, ref 27) at pH 7.1 and $I = 0.105$ (NaCl). ^bCalculated from the data in Table 1 for the unactivated and phosphite-activated reactions of **EO** and **FEO** at pH 7.0 and $I = 0.14$ (NaCl). ^cCalculated from the pD-independent values of k_{ex} for the C-6 deuterium exchange reactions of enzyme-bound **FUMP** (0.041 s^{-1}) and **UMP** ($1.2 \times 10^{-5} \text{ s}^{-1}$) in D_2O at $I = 0.10$ (NaCl) (data from ref 3).

The observed 390-fold effect of a 5-F substituent on the decarboxylation of **EO** can be combined with $k_{\text{cat}} = 15 \text{ s}^{-1}$ for decarboxylation of enzyme-bound **OMP** to estimate a rate constant of $k_{\text{chem}} \approx 6000 \text{ s}^{-1}$ for decarboxylation of enzyme-bound **FOMP** to give enzyme-bound **FUMP** (Scheme 5). This is much larger than the *observed* value of $k_{\text{cat}} = 95 \text{ s}^{-1}$ for **FOMP**,²⁷ and it is consistent with a change in rate-determining step for k_{cat} from the chemical step of loss of CO_2 for **OMP** (k_{chem} , Scheme 5), to product release for the much more reactive substrate **FOMP** (k_{off}).¹⁸ These conclusions are supported by the observations of a substantially smaller primary ^{13}C isotope effect on $k_{\text{cat}}/K_{\text{m}}$ for the decarboxylation of **FOMP** than for **OMP** labeled at the 6-CO_2^- group,²⁸ and of larger dependencies on solvent viscosity of the kinetic parameters $k_{\text{cat}}/K_{\text{m}}$ and k_{cat} for the decarboxylation of **FOMP** than for **OMP**.¹⁸

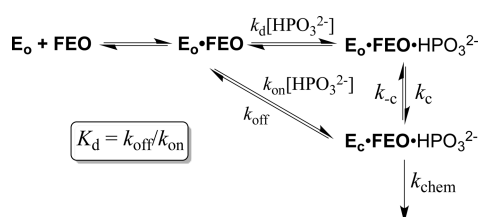
By contrast with the relatively large 390-fold difference in the second-order rate constants for the *unactivated* OMPDC-catalyzed decarboxylation reactions of **EO** and **FEO**, for which the chemical step of the loss of CO_2 from the substrate is

clearly rate-determining, there is only a minimal 4-fold increase in the third-order rate constant (k_{cat}/K_m)_{E•HPI}/ K_d for the phosphite-activated decarboxylation of **EO** upon the addition of a 5-F substituent to give **FEO** (Table 1). This provides strong evidence that, by analogy with the decarboxylation of **FOMP**, the phosphite-activated decarboxylation of **FEO** is not limited by the chemical step of the loss of CO₂ from the substrate. We conclude that the OMPDC-catalyzed reactions of **FOMP** and of the corresponding substrate pieces **FEO** and HPO₃²⁻ are limited by the formation of the reactive binary **E•FOMP** and ternary **E•FEO•HPO₃²⁻** complexes, respectively.

Decarboxylation of FEO Limited by a Conformational Change. We have proposed that OMPDC exists in two forms: a predominant *inactive* loop open form, **E_O**, and a rare *active* loop closed form **E_C**.^{13,17} This conformational change is proposed to result in an environment at the active site that is optimized for catalysis of decarboxylation and deuterium exchange reactions.^{13,17} The conversion of **E_O** to **E_C** involves, at a minimum, closure of the mobile active site loop (loop 7), which sequesters the bound substrate from bulk solvent.^{29–32} There is a large difference between the small *observed* binding energy of HPO₃²⁻ at the free ground state enzyme ($K_d \approx 0.1$ M, Scheme 4 and Figure 1) and the much larger *intrinsic* phosphite binding energy of 7.7 kcal/mol for the phosphite-activated reaction of the truncated substrate **EO** (Table 1). This difference is the binding energy that is specifically utilized to stabilize the transition state for enzyme-catalyzed decarboxylation of **EO**.^{11,13} We have proposed that the large intrinsic phosphite dianion binding energy is utilized to drive the unfavorable conformational change at OMPDC, and at other enzymes, which converts **E_O** to **E_C** and activates the enzyme for catalysis.^{13,17,33–35} Loop closure and the conformational change is driven by the formation of favorable interactions between phosphite dianion and the closed enzyme **E_C**, and this dianion binding energy is expressed later at the transition state for decarboxylation.^{11,13,33}

Scheme 6 shows our proposed kinetic pathway for the phosphite-activated OMPDC-catalyzed decarboxylation of

Scheme 6



FEO. The binding of **FEO** to the ground state open enzyme **E_O** is assumed to precede the binding of HPO₃²⁻, since dianion binding triggers loop closure over the active site and presumably occludes the binding of the second substrate piece.^{29–32} The subsequent binding of phosphite dianion (k_{on}) results in the conformational change and loop closure to give the *productive* ternary Michaelis complex **E_C•FEO•HPO₃²⁻**. The conclusion that the OMPDC-catalyzed decarboxylation of the substrate pieces **FEO** + HPO₃²⁻ is limited by the formation of the reactive ternary **E_C•FEO•HPO₃²⁻** complex (see above) shows that the *chemical* step for decarboxylation of **FEO** is faster than release of phosphite dianion from the enzyme, $k_{\text{chem}} > k_{\text{off}}$ (Scheme 6), so that the binding of phosphite is essentially irreversible. However, this must be reconciled with the

observed *low* affinity of OMPDC for phosphite dianion, $K_d = k_{\text{off}}/k_{\text{on}} \approx 0.1$ M, because weak binding is usually associated with fast ligand release to solution, which would tend to strongly favor a rate-determining chemical step.

Scheme 6 shows that the overall binding of phosphite involves at least two steps: the initial encounter-limited formation of a *weak* complex of HPO₃²⁻ with the **E_O•FEO** complex (k_d), followed by a conformational change (k_c) to give the productive ternary Michaelis complex **E_C•FEO•HPO₃²⁻**. The first-order rate constant for decarboxylation of enzyme-bound **FEO** at the ternary complex can be estimated as $k_{\text{chem}} \leq 6000$ s⁻¹, with the assumption that the decarboxylation of **FEO** should be no faster than the decarboxylation of enzyme-bound **FOMP** (see above). Therefore, the requirement $k_{\text{chem}} > k_{\text{off}}$ and the value of $K_d \approx 0.1$ M (we assume that phosphite binds to **E_O** and **E_O•FEO** with similar affinities) give $k_{\text{on}} \leq 6 \times 10^4$ M⁻¹ s⁻¹ for binding of phosphite dianion to **E_O•FEO** to give the reactive **E_C•FEO•HPO₃²⁻** complex. This *slow* irreversible formation of the reactive ternary complex strongly suggests that the binding of phosphite is limited *not* by diffusional encounter ($k_d \approx 10^7$ M⁻¹ s⁻¹), but rather by the conformational change that results in closure of the loop over the active site (k_c , Scheme 6).

The conclusion that the phosphite-activated decarboxylation of **FEO** is limited by the conformational change that converts the inactive enzyme at the ternary **E_O•FEO•HPO₃²⁻** complex to the active enzyme at the **E_C•FEO•HPO₃²⁻** complex contrasts the observed encounter-limited formation of the reactive **E_C•FOMP** complex with $k_{\text{cat}}/K_m = k_d \approx 1 \times 10^7$ M⁻¹ s⁻¹ (Scheme 5). These results suggest that there is a larger barrier to loop motion and the conformational change at the **E_O•FEO•HPO₃²⁻** complex than at the physiological **E_O•FOMP** complex, resulting in a change in rate-limiting step for the overall decarboxylation from k_d for the reaction of **FOMP** (Scheme 5) to k_c for the *phosphite-activated* reaction of **FEO** (Scheme 6). We suggest that the slower closure of the loop at **E_O•FEO•HPO₃²⁻** than at **E_O•FOMP** results from a higher entropy of activation for the former process, arising from a greater requirement for “freezing” the conformation of weakly bound HPO₃²⁻ at **E_O•FEO•HPO₃²⁻** on proceeding to the tighter **E_C•FEO•HPO₃²⁻** complex.

4'-Substituent Effects. Table 3 summarizes the effects of 4'-CH₂OPO₃²⁻, 4'-CH₂OH, and 4'-CH₃ substituents on the unactivated and the phosphite-activated OMPDC-catalyzed decarboxylation reactions of the truncated substrates **EO** and/or **FEO**.

The large 4×10^8 -fold difference in the second-order rate constants for OMPDC-catalyzed decarboxylation of the natural substrate **OMP** ($k_{\text{cat}}/K_m = 1.1 \times 10^7$ M⁻¹ s⁻¹)⁷ and the truncated substrate **EO** [$(k_{\text{cat}}/K_m)_E = 0.026$ M⁻¹ s⁻¹]¹³ shows that the 4'-CH₂OPO₃²⁻ substituent stabilizes the transition state for decarboxylation by 11.7 kcal/mol.^{7,11,13} However, this large intrinsic phosphite binding energy³⁶ is not fully expressed for the decarboxylation of **FOMP**. Here the *encounter-limited* decarboxylation of **FOMP** (see above) results in only a 1×10^6 -fold difference in the second-order rate constants for the OMPDC-catalyzed decarboxylation reactions of **FOMP** and **FEO**. The observed transition state stabilization from the 4'-CH₂OPO₃²⁻ group of **FOMP** is only 8.3 kcal/mol, which suggests that the barrier to the decarboxylation of **FOMP** is ca. 3.4 kcal/mol lower than that expected if the chemical step were rate-determining. This is consistent with a rate constant ratio of $k_{\text{chem}}/k_{\text{d}} \approx 300$ for partitioning of enzyme-bound **FOMP**

Table 3. Effect of 4'-Substituents on the Decarboxylation Reactions of the Truncated Substrates EO and FEO Catalyzed by Yeast OMPDC at 25 °C

substrate	4'-substituent	effect of 4'-substituent	$\Delta\Delta G^\ddagger$ (kcal/mol)
EO	CH ₂ OPO ₃ ²⁻	+4.2 × 10 ⁸ -fold ^a	-11.7
FEO	CH ₂ OPO ₃ ²⁻	+1.2 × 10 ⁶ -fold ^a	-8.3
EO	CH ₂ OH	-140-fold ^b	+2.9
EO + HPO ₃ ²⁻	CH ₂ OH	-1.3 × 10 ⁶ -fold ^c	+8.3
FEO	CH ₃	-130-fold ^b	+2.9
FEO + HPO ₃ ²⁻	CH ₃	-3000-fold ^c	+4.7

^aCalculated from the values of k_{cat}/K_m for the decarboxylation of OMP (1.1 × 10⁷ M⁻¹ s⁻¹, ref 7) and FOMP (1.2 × 10⁷ M⁻¹ s⁻¹, ref 27) at pH 7.1 and $I = 0.105$ (NaCl) and the values of $(k_{\text{cat}}/K_m)_E$ in Table 1 for the decarboxylation of EO and FEO at pH 7.0 and $I = 0.14$ (NaCl). ^bCalculated from the values of $(k_{\text{cat}}/K_m)_E$ in Table 1 for the unactivated decarboxylation reactions of EO, orotidine, FEO, and 5'-dFO at pH 7.0 or pH 7.1 (for orotidine) and $I = 0.14$ (NaCl). ^cCalculated from the values of $(k_{\text{cat}}/K_m)_{E\cdot\text{HPI}}/K_d$ in Table 1 for the phosphite-activated decarboxylation reactions of EO, FEO, and 5'-dFO at pH 7.0 and $I = 0.14$ (NaCl) and the reaction of orotidine at pH 7.1 and $I = 0.21$ (NaCl).

between decarboxylation and release to solution (Scheme 5). The dependence of k_{cat}/K_m for the decarboxylation of OMP on solvent viscosity is consistent with a partitioning ratio of $k_{\text{chem}}/k_{-d} \approx 0.6$ for the reaction of OMP,¹⁸ which is similar to the reported commitment to catalysis of $k_{\text{cat}}/k_{-d} = 0.3$.⁸ If there is little or no effect of a 5-F substituent on the rate constant k_{-d} for release of the enzyme-bound nucleotide to solution, these observations suggest that there is a ca. 500-fold effect of a 5-F substituent on k_{chem} for decarboxylation of the enzyme-bound nucleotide (Scheme 5). This is very similar to the 400-fold effect of a 5-F substituent on decarboxylation determined directly from the unactivated OMPDC-catalyzed decarboxylation reactions of FEO and EO, for which the chemical step is cleaning rate-limiting (Table 2).

We expected that the phosphodianion binding pocket of OMPDC would easily accommodate the 4'-CH₃ group of 5'-dFO at the transition state for enzyme-catalyzed decarboxylation, because the enzyme has evolved to accommodate the presumably even larger 4'-CH₂OPO₃²⁻ group of OMP. We were therefore very surprised to find that the addition of a 4'-CH₃ group to FEO to give 5'-dFO results in a substantial 130-fold decrease in the rate constant for the unactivated decarboxylation and a 2.9 kcal/mol destabilization of the transition state (Table 3). There is an even larger 3000-fold effect (4.7 kcal/mol transition state destabilization) of the addition of a 4'-CH₃ group to FEO to give 5'-dFO on the third-order rate for the phosphite-activated reactions of these substrates. Therefore, not surprisingly, the steric effect of the 4'-CH₃ group on decarboxylation at the ternary E•5'-dFO•HPO₃²⁻ complex is larger than that at the binary E•5'-dFO complex.

Interestingly, the 4'-CH₂OH group of orotidine results in the same 2.9 kcal/mol destabilization of the transition state for decarboxylation observed for the 4'-CH₃ group of 5'-dFO, and there are similar stabilizations of the transition states for these reactions by the binding of phosphite dianion of 2.3 and 3.2 kcal/mol, respectively (Table 1). This suggests that there is little contribution of the terminal 5'-OH group of orotidine to the stability of the transition state for decarboxylation. By contrast, the 4'-CH₂OH group of orotidine results in a very

large 8.3 kcal/mol destabilization of the transition state for phosphite-activated decarboxylation, exceeding the destabilization observed for the 4'-CH₃ group of 5'-dFO by 3.6 kcal/mol (Table 3). The destabilization of the transition state for the latter is masked because the reactivity of the parent two-part substrate FEO + phosphite is attenuated by the rate-limiting conformational change (see above).

These surprisingly large 4'-CH₃ and 4'-CH₂OH substituent effects on the decarboxylation reactions of FEO and EO are consistent with destabilization of the transition state for decarboxylation by steric effects of these groups that disrupt the required precise positioning of the peptide backbone and amino acid side chains at the reactive closed form of OMPDC. This is consistent with our earlier proposal that the binding energy of the substrate phosphodianion group is utilized to stabilize a rare active closed form of OMPDC that is required for the decarboxylation of both whole and truncated substrates.^{13,17,25,35}

AUTHOR INFORMATION

Corresponding Author

*Tel: (716) 645 4232. Fax: (716) 645 6963. E-mail: jrichard@buffalo.edu.

Funding

This work was supported by Grant GM39754 from the National Institutes of Health.

Notes

The authors declare no competing financial interest.

ACKNOWLEDGMENTS

We thank Professor Steven Diver for helpful discussions regarding the synthesis of FEO and 5'-dFO.

ABBREVIATIONS USED

OMPDC, orotidine 5'-monophosphate decarboxylase; OMP, orotidine 5'-monophosphate; UMP, uridine 5'-monophosphate; FOMP, 5-fluoroorotidine 5'-monophosphate; FUMP, 5-fluorouridine 5'-monophosphate; EO, 1-(β-D-erythrofuransyl)orotic acid; EU, 1-(β-D-erythrofuransyl)-uracil; FEO, 1-(β-D-erythrofuransyl)-5-fluoroorotic acid; FEU, 1-(β-D-erythrofuransyl)-5-fluorouracil; 5'-dFO, 5'-deoxy-5-fluoroorotidine; 5'-dFU, 5'-deoxy-5-fluorouridine; LDA, lithium diisopropylamide; BuLi, butyllithium; THF, tetrahydrofuran; MOPS, 3-(N-morpholino)propanesulfonic acid; NMR, nuclear magnetic resonance

REFERENCES

- (1) Radzicka, A., and Wolfenden, R. (1995) A proficient enzyme. *Science* 267, 90–93.
- (2) Miller, B. G., and Wolfenden, R. (2002) Catalytic proficiency: the unusual case of OMP decarboxylase. *Annu. Rev. Biochem.* 71, 847–885.
- (3) Tsang, W.-Y., Wood, B. M., Wong, F. M., Wu, W., Gerlt, J. A., Amyes, T. L., and Richard, J. P. (2012) Proton Transfer from C-6 of Uridine 5'-Monophosphate Catalyzed by Orotidine 5'-Monophosphate Decarboxylase: Formation and Stability of a Vinyl Carbanion Intermediate and the Effect of a 5-Fluoro Substituent. *J. Am. Chem. Soc.* 134, 14580–14594.
- (4) Toth, K., Amyes, T. L., Wood, B. M., Chan, K., Gerlt, J. A., and Richard, J. P. (2010) Product Deuterium Isotope Effects for Orotidine 5'-Monophosphate Decarboxylase: Effect of Changing Substrate and Enzyme Structure on the Partitioning of the Vinyl Carbanion Reaction Intermediate. *J. Am. Chem. Soc.* 132, 7018–7024.

- (5) Amyes, T. L., Wood, B. M., Chan, K., Gerlt, J. A., and Richard, J. P. (2008) Formation and Stability of a Vinyl Carbanion at the Active Site of Orotidine 5'-Monophosphate Decarboxylase: pK_a of the C-6 Proton of Enzyme-Bound UMP. *J. Am. Chem. Soc.* 130, 1574–1575.
- (6) Toth, K., Amyes, T. L., Wood, B. M., Chan, K., Gerlt, J. A., and Richard, J. P. (2007) Product Deuterium Isotope Effect for Orotidine 5'-Monophosphate Decarboxylase: Evidence for the Existence of a Short-Lived Carbanion Intermediate. *J. Am. Chem. Soc.* 129, 12946–12947.
- (7) Toth, K., Amyes, T. L., Wood, B. M., Chan, K. K., Gerlt, J. A., and Richard, J. P. (2009) An Examination of the Relationship between Active Site Loop Size and Thermodynamic Activation Parameters for Orotidine 5'-Monophosphate Decarboxylase from Mesophilic and Thermophilic Organisms. *Biochemistry* 48, 8006–8013.
- (8) Porter, D. J. T., and Short, S. A. (2000) Yeast Orotidine 5'-Phosphate Decarboxylase: Steady-State and Pre-Steady-State Analysis of the Kinetic Mechanism of Substrate Decarboxylation. *Biochemistry* 39, 11788–11800.
- (9) Jencks, W. P. (1975) Binding Energy, Specificity and Enzymic Catalysis: The Circe Effect. *Adv. Enzymol. Relat. Areas Mol. Biol.* 43, 219–410.
- (10) Amyes, T. L., and Richard, J. P. Specificity in Transition State Binding: The Pauling Model Revisited, in preparation.
- (11) Amyes, T. L., Richard, J. P., and Tait, J. J. (2005) Activation of orotidine 5'-monophosphate decarboxylase by phosphite dianion: The whole substrate is the sum of two parts. *J. Am. Chem. Soc.* 127, 15708–15709.
- (12) Barnett, S. A., Amyes, T. L., Wood, B. M., Gerlt, J. A., and Richard, J. P. (2008) Dissecting the Total Transition State Stabilization Provided by Amino Acid Side Chains at Orotidine 5'-Monophosphate Decarboxylase: A Two-Part Substrate Approach. *Biochemistry* 47, 7785–7787.
- (13) Amyes, T. L., Ming, S. A., Goldman, L. M., Wood, B. M., Desai, B. J., Gerlt, J. A., and Richard, J. P. (2012) Orotidine 5'-monophosphate decarboxylase: Transition state stabilization from remote protein-phosphodianion interactions. *Biochemistry* 51, 4630–4632.
- (14) Chan, K. K., Wood, B. M., Fedorov, A. A., Fedorov, E. V., Imker, H. J., Amyes, T. L., Richard, J. P., Almo, S. C., and Gerlt, J. A. (2009) Mechanism of the Orotidine 5'-Monophosphate Decarboxylase-Catalyzed Reaction: Evidence for Substrate Destabilization. *Biochemistry* 48, 5518–5531.
- (15) Amyes, T. L., and Richard, J. P. (1996) Determination of the pK_a of Ethyl Acetate: Brønsted Correlation for Deprotonation of a Simple Oxygen Ester in Aqueous Solution. *J. Am. Chem. Soc.* 118, 3129–3141.
- (16) Richard, J. P., and Amyes, T. L. (2001) Proton transfer at carbon. *Curr. Opin. Chem. Biol.* 5, 626–633.
- (17) Goryanova, B., Amyes, T. L., Gerlt, J. A., and Richard, J. P. (2011) OMP Decarboxylase: Phosphodianion Binding Energy Is Used To Stabilize a Vinyl Carbanion Intermediate. *J. Am. Chem. Soc.* 133, 6545–6548.
- (18) Wood, B. M., Chan, K. K., Amyes, T. L., Richard, J. P., and Gerlt, J. A. (2009) Mechanism of the Orotidine 5'-Monophosphate Decarboxylase-Catalyzed Reaction: Effect of Solvent Viscosity on Kinetic Constants. *Biochemistry* 48, 5510–5517.
- (19) Barnett, S. A., Amyes, T. L., McKay Wood, B., Gerlt, J. A., and Richard, J. P. (2010) Activation of R235A Mutant Orotidine 5'-Monophosphate Decarboxylase by the Guanidinium Cation: Effective Molarity of the Cationic Side Chain of Arg-235. *Biochemistry* 49, 824–826.
- (20) Sievers, A., and Wolfenden, R. (2005) The effective molarity of the substrate phosphoryl group in the transition state for yeast OMP decarboxylase. *Bioorg. Chem.* 33, 45–52.
- (21) Bello, A. M., Konforte, D., Poduch, E., Furlonger, C., Wei, L., Liu, Y., Lewis, M., Pai, E. F., Paige, C. J., and Kotra, L. P. (2009) Structure-activity relationships of orotidine-5'-monophosphate decarboxylase inhibitors as anticancer agents. *J. Med. Chem.* 52, 1648–1658.
- (22) Wang, Y., and Burton, D. J. (2006) A Facile, General Synthesis of 3,4-Difluoro-6-substituted-2-pyrones. *J. Org. Chem.* 71, 3859–3862.
- (23) Moffatt, J. G. (1963) The synthesis of orotidine 5'-phosphate. *J. Am. Chem. Soc.* 85, 1118–1123.
- (24) Gasteiger, E., Gattiker, A., Hoogland, C., Ivanyi, I., Appel, R. D., and Bairoch, A. (2003) ExPASy: The proteomics server for in-depth protein knowledge and analysis. *Nucleic Acids Res.* 31, 3784–3788.
- (25) Desai, B. J., Wood, B. M., Fedorov, A. A., Fedorov, E. V., Goryanova, B., Amyes, T. L., Richard, J. P., Almo, S. C., and Gerlt, J. A. (2012) Conformational changes in orotidine 5'-monophosphate decarboxylase: A structure-based explanation for how the 5'-phosphate group activates the enzyme. *Biochemistry* 51, 8665–8678.
- (26) Hupe, D. J., and Jencks, W. P. (1977) Nonlinear Structure-Reactivity Correlations. Acyl Transfer between Sulfur and Oxygen Nucleophiles. *J. Am. Chem. Soc.* 99, 451–464.
- (27) Barnett, S. A. (2009) Studies on the Mechanism of Action of Orotidine 5'-Monophosphate Decarboxylase, Ph.D. Thesis, University at Buffalo, Buffalo, NY.
- (28) Van Vleet, J. L., Reinhardt, L. A., Miller, B. G., Sievers, A., and Cleland, W. W. (2008) Carbon isotope effect study on orotidine 5'-monophosphate decarboxylase: support for an anionic intermediate. *Biochemistry* 47, 798–803.
- (29) Wu, N., Mo, Y., Gao, J., and Pai, E. F. (2000) Electrostatic stress in catalysis: structure and mechanism of the enzyme orotidine monophosphate decarboxylase. *Proc. Natl. Acad. Sci. U. S. A.* 97, 2017–2022.
- (30) Miller, B. G., Hassell, A. M., Wolfenden, R., Milburn, M. V., and Short, S. A. (2000) Anatomy of a proficient enzyme: the structure of orotidine 5'-monophosphate decarboxylase in the presence and absence of a potential transition state analog. *Proc. Natl. Acad. Sci. U. S. A.* 97, 2011–2016.
- (31) Harris, P., Poulsen, J.-C. N., Jensen, K. F., and Larsen, S. (2000) Structural Basis for the Catalytic Mechanism of a Proficient Enzyme: Orotidine 5'-Monophosphate Decarboxylase. *Biochemistry* 39, 4217–4224.
- (32) Begley, T. P., Appleby, T. C., and Ealick, S. E. (2000) The structural basis for the remarkable catalytic proficiency of orotidine 5'-monophosphate decarboxylase. *Curr. Opin. Struct. Biol.* 10, 711–718.
- (33) Richard, J. P. (2012) A Paradigm for Enzyme-Catalyzed Proton Transfer at Carbon: Triosephosphate Isomerase. *Biochemistry* 51, 2652–2661.
- (34) Malabanan, M. M., Amyes, T. L., and Richard, J. P. (2010) A role for flexible loops in enzyme catalysis. *Curr. Opin. Struct. Biol.* 20, 702–710.
- (35) Tsang, W.-Y., Amyes, T. L., and Richard, J. P. (2008) A Substrate in Pieces: Allosteric Activation of Glycerol 3-Phosphate Dehydrogenase (NAD⁺) by Phosphite Dianion. *Biochemistry* 47, 4575–4582.
- (36) Morrow, J. R., Amyes, T. L., and Richard, J. P. (2008) Phosphate Binding Energy and Catalysis by Small and Large Molecules. *Acc. Chem. Res.* 41, 539–548.